

Published in final edited form as:

FEBS Lett. 2014 December 20; 588(24): 4551–4560. doi:10.1016/j.febslet.2014.10.023.

## GABA-A receptor-dependent mechanisms prevent excessive spine elimination during postnatal maturation of the mouse cortex *in vivo*

Yachi Chen<sup>1</sup>

<sup>1</sup>Department of Neurobiology and Behavior and Center for Nervous System Disorders, State University of New York at Stony Brook, Stony Brook, NY 11794

### Abstract

Dendritic spine dynamics are implicated in the structural plasticity of cognition-related neuroconnectivity. This study utilized the transcranial *in vivo* imaging approach to investigate spine dynamics in intact brains of living yellow fluorescent protein-expressing mice. A developmental switch in the net spine loss rate occurred at ~4 months of age. The initially rapid rate slowed down ~6-fold due to substantially reduced spine elimination with minor changes in formation. Furthermore, pharmacological blockade of  $\gamma$ -aminobutyric acid type A (GABA-A) receptors resulted in significantly increased elimination of pre-existing spines without affecting new spine formation. Spine elimination returned to normal levels following treatment cessation. Thus, GABA-A receptor-dependent mechanisms act as “brakes” – keeping spine elimination in check to prevent over-pruning, thereby preserving the integrity of cognition-related cortical circuits.

### Keywords

bicuculline; cortex; dendritic spines; GABA-A receptor; development

### Introduction

The neocortex receives a majority of excitatory glutamatergic inputs via synaptic contacts made on dendritic spines, which are small membranous protrusions along the dendrites of pyramidal neurons. Thus, spines are major postsynaptic contact sites of glutamatergic synapses within cortical circuits. Spines are believed to facilitate synaptic throughput of excitatory signals to dendritic branches for information processing and to compartmentalize synaptic proteins for a synapse-specific response (see [1–8] for recent reviews). Spines are dynamic structures that appear and disappear within the neuronal circuitry. Spine dynamics,

© 2014 Elsevier B.V. on behalf of the Federation of European Biochemical Societies. All rights reserved.

Corresponding author: Dr. Yachi Chen, Department of Neurobiology and Behavior and Center for Nervous System Disorders, State University of New York at Stony Brook, Stony Brook, NY 11794. yachi.chen@stonybrook.edu.

**Publisher's Disclaimer:** This is a PDF file of an unedited manuscript that has been accepted for publication. As a service to our customers we are providing this early version of the manuscript. The manuscript will undergo copyediting, typesetting, and review of the resulting proof before it is published in its final citable form. Please note that during the production process errors may be discovered which could affect the content, and all legal disclaimers that apply to the journal pertain.

i.e., the dynamic changes in the lifespan of spines, result in synaptic rearrangements implicated in learning and memory throughout life. Indeed, many previous *in vivo* studies have linked changes in spine turnover to activity-dependent sensory or visual experience and behavioral learning processes [9–15].

In humans, the density of spines on cortical pyramidal neurons changes throughout postnatal development. The spine density peaks between ages 7 and 9 and then declines substantially during late childhood and adolescence (9–22 years) [16–18]. The spine density continues to decrease well into the 30s and becomes stabilized after 40 years of age [16–18]. Thus, considerable circuit refinement occurs from late childhood to mid-adulthood. These changes in spine density during postnatal circuit maturation are thought to reflect learning capacity at critical developmental time periods and stabilization of connectivity in maturity for memory retention. Furthermore, the spine density at a given stage of development is determined by the rates of active spine elimination and formation. To understand how optimal levels of stable spine-based synaptic connectivity are maintained throughout postnatal development, it is therefore essential to investigate the neural mechanisms that modulate spine turnover during circuit maturation.

The ionotropic  $\gamma$ -aminobutyric acid type A (GABA-A) receptor consists of five pore-forming subunits, which assemble into a GABA-gated chloride channel. GABA-A receptors can either depolarize or hyperpolarize a neuron depending on the developmentally regulated expression of the chloride transporters, NKCC1 and KCC2 [19, 20]. NKCC1 is mainly expressed from the embryonic stage until the first postnatal week of development. Moreover, NKCC1 imports chloride ions and increases intracellular chloride concentrations in immature neurons. Due to high intracellular chloride concentrations, GABA-A receptor activation typically causes chloride ions to move outward, resulting in depolarization early in development. This GABA-A receptor-mediated excitatory response affects the processes of DNA synthesis, cell proliferation, migration, maturation of excitatory synapses and dendritic morphology, and spine formation during early development of cortical circuitry [21–25]. Following birth, the expression of KCC2 transporters is up-regulated. The chloride pumping action of KCC2 lowers intracellular chloride concentrations in more mature neurons. GABA binding to GABA-A receptor results in chloride ion influx, hyperpolarization of neurons, and the generation of inhibitory activity that dampens postsynaptic excitability and prevents neuronal firing [26–28]. GABA-A receptors mediate two types of inhibition, i.e., synaptic (phasic) and extrasynaptic (tonic) inhibition. GABA-A receptors localized to synaptic sites are exposed to brief, saturating levels of GABA and mediate “phasic” inhibition. Following GABA binding, these synaptic GABA-A receptors generate fast and precisely timed inhibition in the form of inhibitory postsynaptic currents [26]. This “phasic” inhibition provides a rapid point-to-point communication in establishing the temporal window for synaptic integration and neuronal network oscillation [29, 30]. In contrast, extrasynaptic GABA-A receptors are localized to sites displaced from GABA release and they mediate “tonic” inhibition. These receptors are activated by low concentrations of ambient GABA present in the extracellular space from synaptic spillover or non-vesicular release. Activation of extrasynaptic GABA-A receptors generates an uninterrupted, “tonic” conductance that maintains a constant level of inhibition of neuronal

excitability [26, 31, 32]. The subunit composition of the final assembly affects the synaptic or extrasynaptic localization of GABA-A receptors within a neuron [33]. The inhibitory action of synaptic and extrasynaptic GABA-A receptors controls many neuronal processes, including the proliferation and migration of neuroblasts, synapse formation, and synaptic plasticity essential for neuronal development and functioning. GABA-A receptors function beyond chloride channels that regulate membrane potential and conductance. GABA-A receptors have been shown to affect protein phosphorylation and intracellular calcium concentrations, which are critical to brain development and neurogenesis [34, 35]. Moreover, the interaction of the GABA-A receptor with synaptic adhesion molecules might provide structural functions in the maturation and stabilization of GABAergic synapses [36, 37]. Taken together, the GABA-A receptor acts beyond its classical role in synaptic inhibition.

In pyramidal neurons, GABA-A receptors are prevalent in the somatodendritic compartment, including spines. GABAergic inhibitory synapses that target spines have been shown to exert highly focal inhibition of calcium transients and excitatory postsynaptic potentials within individual spines [38]. Thus, activation of GABA receptors inhibits the calcium and electrical response within individual spines in a highly spatially precise manner. In the cat visual cortex, ~93% of inhibitory synapses targeting excitatory pyramidal neurons terminate on dendrites and spines [39]. Given the large proportion of inhibitory synapses targeting dendrites and spines, it is likely that GABA-A receptors are ideally situated on dendrites and spines to directly modulate spine turnover via localized control of dendritic activity and biochemical signaling. However, the contribution of GABA-A receptor-mediated synaptic inhibition in long-term spine dynamics during cortical circuit refinement remains unclear.

To provide a rigorous assessment of the developmental changes in spine dynamics and to investigate GABA-A receptor-dependent mechanisms in the modulation of spine turnover during postnatal circuit maturation, I utilized a high-resolution, two photon-based transcranial *in vivo* imaging approach to repeatedly visualize bio-fluorescently labeled postsynaptic contact sites, i.e., spines, in the intact brains of living mice under pharmacological manipulations.

## Results

### Repeated long-term *in vivo* imaging demonstrates a nearly 6-fold reduction in the rate of net spine loss in maturity

To study the developmental changes in spine turnover that underlie postnatal circuit refinement in the mammalian neocortex, I investigated the degree of spine elimination and formation *in vivo* in transgenic mice, which express yellow fluorescent protein (YFP) in excitatory pyramidal neurons located in the deep cortical layer V. YFP expression labels layer V pyramidal neurons in its entirety, thereby allowing visualization of minute structures, such as spines. Two photon-excitation laser scanning microscopy using a “thinned-skull” cranial viewing window is a repeated, high-resolution live imaging approach that is well suited for exploring the structural dynamics of spine-based excitatory synapses *in vivo* (Fig 1A–E; see also Materials and Methods). The “thinned-skull” method involves

reducing the skull thickness to ~20 – 30  $\mu\text{m}$ . In contrast to traditional craniotomy, the skull remains intact after the procedure, which minimizes post-surgical inflammatory responses in the brain. Through the “thinned-skull” window, I repeatedly visualized, in exquisite detail, spines on the distal portion (i.e., within cortical layer I) of apical dendrites of YFP-expressing layer V pyramidal neurons in living mice (Fig 1E). This method enables the investigation of the *in vivo* temporal and spatial dynamics of spines over weeks and months. Previously, serial section immunoelectron microscopy studies performed following *in vivo* imaging of spines of YFP-labeled pyramidal neurons have shown that all re-identified spines bear synaptic contacts [40]. Thus, YFP-labeled spines imaged *in vivo* closely represent excitatory synapses.

Recent findings from the human cortex have demonstrated that the spine density of pyramidal neurons rapidly declines starting from late childhood [18]. This decreasing trend continues into adolescence, but begins to slow down substantially in late adolescence [18]. A rigorous assessment of dynamic changes in spine elimination and formation during critical time periods is essential to our understanding of the developmental regulation of spine density, which is fundamentally important to the integrity of spine-base synaptic connectivity. To provide information on the degree of spine elimination and formation during postnatal development, I re-imaged 1-month-old mice after one day, one week or 3 months to establish short- and long-term spine dynamics profiles during the first 4 postnatal months of circuit maturation (see Materials and Methods for further details on time lapse studies). In addition, I re-imaged 4-month-old animals after one week or 6 months to study spine turnover in maturity.

In the present study, a total of 10,115 distinct dendritic spines in the primary somatosensory cortex were tracked and analyzed over two imaging sessions. Upon initial inspection, spine dynamics appeared to be associated with the maturation stage of cortical circuitry because more spines had undergone turnover in 1-month-old animals than in 4-month-old mice (Fig 2A). Further image analyses revealed interesting changes in the dynamic profiles of spines between the two distinct time windows under study (i.e., from 1 month to 4 months of age vs. from 4 months to 10 months of age). In 1-month-old animals (age:  $29.42 \pm 0.38$  days), I found that the percentage of eliminated spines increased gradually but significantly as the imaging time interval was extended from 1 day, to 1 week, or to 3 months (1 day:  $3.40 \pm 0.46\%$  from  $n=4$  mice; 1 week:  $9.63 \pm 0.69\%$  from  $n=6$  mice; 3 months:  $20.27 \pm 0.96\%$  from  $n=3$  mice; Fig 2B). Similarly, the percentage of newly added spines increased over time (1 day:  $2.81 \pm 0.52\%$  from  $n=4$  mice; 1 week:  $5.76 \pm 0.42\%$  from  $n=6$  mice; 3 months:  $7.68 \pm 0.75\%$  from  $n=3$  mice; Fig 2B), although to a lesser degree than spine elimination. Because the proportion of eliminated spines was significantly higher than added spines over the 1-week or 3-months period, there was a gradual net loss of spines as 1-month-old mice matured into approximately 4 months of age in late adolescence/early adulthood (Fig 2B). Additional experiments in older animals showed that this gradual loss of spines continued in maturity. In 4-month-old animals (age:  $4.19 \pm 0.11$  months), the percentage of eliminated spines increased significantly from  $4.46 \pm 0.44\%$  ( $n=4$  mice) over a 1-week interval to  $14.27 \pm 0.74\%$  ( $n=4$  mice) over a 6-month interval (Fig 2C). Thus, the substantial elimination of pre-existing spines occurred as 4-month-old mice matured into 10 months of age in mid-

adulthood. Four-month-old animals also formed new spines during maturation. They showed a significant increase in the percentage of newly formed spines, from  $4.35 \pm 0.68\%$  ( $n=4$  mice) over a 1-week period to  $10.14 \pm 0.66\%$  ( $n=4$  mice) over a 6-month period (Fig 2C). Although 4-month-old mice showed comparable levels of spine elimination and formation with no net loss of spines over the short-term, chronic high-resolution *in vivo* imaging revealed a significantly greater proportion of spines eliminated compared to spines added, resulting in a net spine loss over the long-term period. On the basis of these results, the net loss of spines persists for a prolonged period of time during postnatal circuit maturation in the mouse cortex. However, a large decrease in the proportion of eliminated spines after the first 4 postnatal months results in a smaller net loss of spines in maturity.

To obtain a deeper understanding of the extent of changes in the structural stability of excitatory circuits during synaptic refinement, I determined the fraction of spines that survived by the end of each time frame (or the survival fraction). Relative to the initial total spine number, 1-month-old mice had  $96.13 \pm 1.02\%$  ( $n=6$  mice) of spines, whereas 4-month-old animals had an even larger proportion of spines, i.e.,  $99.89 \pm 0.87\%$  ( $n=4$  mice) after one week (Fig 2D). Over the long-term period, 1-month-old mice had  $87.41 \pm 0.70\%$  spines ( $n=3$  mice) after 3 months, whereas 4-month-old animals had  $95.87 \pm 0.92\%$  ( $n=4$  mice) after 6 months (Fig 2D). The proportion of spines survived over either the short- or long-term was significantly greater in 4-month-old animals compared to younger mice. Thus, spines became more persistent as the animals matured, contributing to the increased stability of cortical excitatory circuits in maturity. Intriguingly, 4-month-old animals lost spines at a rate of 0.69% per month, versus 3.99% per month in 1-month-old animals (Fig 2D; calculated slopes of the regression lines from the linear regression analysis). These findings demonstrated that after the first 4 postnatal months, the rate of net spine loss decreases approximately 6-fold.

Taken together, results from this study were consistent with the idea that while a majority of spines persist for long periods, a proportion of spines undergo turnover, with more pre-existing spines being eliminated than new spines being added, resulting in a net loss of spines in the postnatal development of the mouse cortex. The initially rapid rate of net spine loss slows down by approximately 6-fold starting at ~4 months of age, a time thought to correlate to the transition from late adolescence to young adulthood in humans [41]. This dramatic switch in the net spine loss rate is critical to the structural stability of excitatory circuits in maturity.

### **GABA-A receptor-dependent mechanisms keep spine elimination in check to promote circuit integrity**

The results presented thus far have shown that spine elimination occurs more extensively than formation, resulting in a net loss of spines during the prolonged period of postnatal circuit maturation in mice. Although the net spine loss occurs rapidly in the first 4 postnatal months, the rate of net spine loss decelerates nearly 6-fold in maturity due to significantly reduced spine elimination. Thus, the elimination of pre-existing spines is closely modulated throughout the period of circuit refinement. Given the extensiveness of the developmental modulation of spine elimination, regulatory mechanisms must be established to keep spine

elimination in check to prevent excessive spine loss during brain maturation. These mechanisms are presumably critically important for maintaining normal levels of stable spine-based synaptic connections and promoting the overall integrity of neuronal networks. Malfunction of such control mechanisms is expected to cause over-pruning of spines and decreased stability of synaptic connectivity, thereby jeopardizing the integrity of cortical circuitry. Thus, I began to explore mechanisms that modulate spine turnover in synaptic refinement. Recently, an interesting *in vivo* study of inhibitory synapses in the neocortex demonstrated that dynamic inhibitory synapses (i.e., inhibitory synapses that undergo elimination or formation over a time frame) are in closer proximity to dynamic spines compared to stable spines along the same dendritic segment [40]. This spatial clustering of dynamic inhibitory synapses with dynamic spines along the same dendrite implicates a role for GABAergic inhibitory tone in spine dynamics. Intrigued by this unique spatial coordination, I investigated whether GABA-A receptors, which mediate GABAergic inhibition in mature neurons, may function in spine turnover.

To explore the effects of GABA-A receptors on spine dynamics, I administered daily injections of bicuculline methiodide, a GABA-A receptor antagonist, to 1-month-old YFP-expressing mice (age:  $30.17 \pm 0.30$  days) and analyzed the proportion of spine eliminated or added over the short-term. Interestingly, bicuculline treatment resulted in a significant increase in the percentage of eliminated spines compared to saline treatment (eliminated:  $10.75 \pm 0.88\%$  in  $n=6$  saline-injected mice vs.  $16.45 \pm 1.25\%$  in  $n=6$  bicuculline-injected mice over  $9.08 \pm 0.84$  days; Fig 3A). However, bicuculline had no significant effects on the percentage of newly added spines over the same time duration (added:  $6.12 \pm 0.34\%$  in  $n=6$  saline-injected mice vs.  $6.68 \pm 0.66\%$  in  $n=6$  bicuculline-injected mice; Fig 3A). Bicuculline treatment resulted in a greater net loss of spines compared to the control treatment due to a larger fraction of eliminated spines (Fig 3A). To determine whether bicuculline enhancement of spine elimination is specific to a critical period in circuit refinement, I subsequently expanded the study and investigated the bicuculline effects in older animals. In 5-month-old animals (age:  $5.05 \pm 0.13$  months), bicuculline treatment significantly increased the percentage of eliminated spines (eliminated:  $3.90 \pm 0.29\%$  in  $n=5$  saline-injected mice vs.  $7.78 \pm 0.78\%$  in  $n=5$  bicuculline-injected mice over  $10.60 \pm 1.07$  days; Fig 3B). Consistent with the results in 1-month-old mice, bicuculline did not significantly affect the percentage of newly added spines in 5-month-old animals (added:  $3.40 \pm 0.86\%$  in  $n=5$  saline-injected mice vs.  $4.34 \pm 1.21\%$  in  $n=5$  bicuculline-injected mice; Fig 3B). Thus, bicuculline treatment resulted in the excessive elimination of pre-existing spines, thereby leading to a net loss of spines even in maturity (Fig 3B). My findings clearly demonstrated that functional perturbation of GABA-A receptors with bicuculline enhanced spine elimination without affecting spine formation, and this resulted in accelerated spine loss. Moreover, the specific increase in spine elimination from bicuculline administration occurred within a broad developmental time frame demonstrating the breadth of bicuculline effects during postnatal brain maturation. These data provide strong evidence supporting a critical GABA-A receptor function in preventing spine over-pruning during network refinement.

Next, I studied whether the cessation of bicuculline injections in bicuculline-treated animals could return spine elimination to normal levels, which would demonstrate that enhanced spine elimination specifically results from GABA-A receptor blockade. Expectedly, in animals receiving daily bicuculline injections prior to the final imaging session, the percentage of eliminated spines was significantly greater than that of age-matched control mice (eliminated:  $5.85 \pm 0.63\%$  in  $n=4$  saline-injected mice vs.  $13.34 \pm 0.83\%$  in  $n=5$  bicuculline-injected mice at  $53.11 \pm 1.95$  days of age over  $8.67 \pm 0.76$  days; Fig 3C). Intriguingly, withdrawal of bicuculline in bicuculline-treated animals resulted in percentage of spine elimination that were comparable to that of age-matched control animals, which were subjected to the same experimental paradigm with saline (eliminated:  $6.87 \pm 1.26\%$  in  $n=3$  saline-withdrawal mice vs.  $6.10 \pm 1.10\%$  in  $n=3$  bicuculline-withdrawal mice at  $56.67 \pm 2.64$  days of age over 14 days; Fig 3C). Thus, the cessation of bicuculline treatment returned spine elimination to normal levels. For spine formation, the percentage of newly added spines in bicuculline-treated animals (added:  $3.45 \pm 0.60\%$  in  $n=4$  saline-injected mice vs.  $3.52 \pm 0.57\%$  in  $n=5$  bicuculline-injected mice at  $53.11 \pm 1.95$  days of age over  $8.67 \pm 0.76$  days; Fig 3C) and bicuculline-treated mice later subjected to bicuculline withdrawal (added:  $4.70 \pm 0.52\%$  in  $n=3$  saline-withdrawal mice vs.  $3.93 \pm 0.35\%$  in  $n=3$  bicuculline-withdrawal mice at  $56.67 \pm 2.64$  days of age over 14 days; Fig 3C) was not significantly different from that of age-matched control animals. Consistent with my previous findings, bicuculline did not affect new spine formation. Taken together, spine elimination was enhanced following bicuculline administration and subsequently returned to normal levels upon treatment cessation. This reversibility clearly indicated that enhanced spine elimination specifically results from GABA-A receptor blockade by bicuculline.

To provide a further understanding of the GABA-A receptor's effects on the structural stability of cortical circuits, I determined the fraction of surviving spines following bicuculline inhibition of GABA-A receptor activation. I found that bicuculline-treated animals had a significantly smaller survival fraction of spines than age-match saline-treated animals ( $97.34 \pm 0.67\%$  of spines retained over  $9.47 \pm 0.82$  days in  $n=15$  saline-injected mice vs.  $92.19 \pm 0.95\%$  of spines retained over  $9.31 \pm 0.74$  days in  $n=16$  bicuculline-injected mice; age range: 29 days to 5.5 months; Fig 3D). Thus, bicuculline blockade of GABA-A receptor activation results in decreased spine survival over time, which indicates a less stable cortical excitatory circuitry. In conclusion, activation of GABA-A receptors curtails spine elimination to prevent excessive pruning of pre-existing spines, thereby promoting normal levels of stable spine-based synaptic connections during postnatal circuit refinement.

## Discussion

Using transcranial two photon-excitation laser scanning microscopy, the present *in vivo* study examined developmental changes in spine turnover during postnatal circuit refinement in the mouse cortex. Furthermore, the study investigated the role of GABA-A receptors in the modulation of spine elimination. This study provided three main *in vivo* findings. First, the substantial decline in spine number during circuit refinement is not due to the decreased formation of new spines. Instead, the elimination of the pre-existing spines occurs more extensively than spine formation as the circuit matures, and this finding represents the

predominant mechanism for the sustained net loss of spines that persists into adulthood. Second, spine elimination decreases substantially after the first 4 postnatal months, which contributes to an approximately 6-fold reduction in the rate of net spine loss, culminating in the structural stability of mature circuits. Third, disruption of GABA-A receptor activation results in an excessive elimination of pre-existing spines without affecting the formation of new spines, which demonstrates GABA-A receptor function in preventing spine over-pruning during the prolonged period of synaptic refinement in the mouse cortex.

### **The initially rapid rate of net spine loss slows down nearly 6-fold in maturity**

Previous postmortem analyses of spine density in humans have revealed extensive loss of spines between the ages of 9 to 22, which encompasses late childhood and adolescence, and this decrease in the spine density continues beyond adolescence into adulthood until 40 years of age, after which the spine density becomes stabilized [16–18]. Here, my *in vivo* data from the mouse cortex indicated that this substantial decline in spine number most likely results from an extensive elimination of pre-existing spines within cortical circuits and is not due to a decreased proportion of newly added spines in mice. Furthermore, I found that as circuits mature beyond the first 4 postnatal months, active spine elimination continues to exceed spine formation. Hence, the net loss of spines persists into adulthood. This extended period of postnatal regulation of spine turnover during circuit maturation is consistent with previous developmental profiles of spine density in humans. Most importantly, this study revealed a developmental switch in the rate of net spine loss, which decreases nearly 6-fold after the first 4 postnatal months. This considerable slowing down in the net spine loss rate is crucial for the overall stabilization of spine-based synaptic connectivity in adulthood. Thus, findings obtained from humans and rodents support the notion that in postnatal cortical circuit maturation, a net spine loss occurs over an extended time period and continues into adulthood when active elimination of pre-existing spines exceeds the formation of new spines. However, a nearly 6-fold decrease in the net spine loss rate starting from late adolescence/early adulthood ensures that a large proportion of spines is stably integrated within the adult brain.

### **GABA-A receptor-dependent mechanisms curtail spine elimination to prevent excessive spine loss during circuit maturation**

The assembly and refinement of neural circuits are known to involve neuronal activity-dependent mechanisms. Previous *in vivo* imaging studies strongly support a role for neuronal activity in experience- and learning-induced structural plasticity of cortical circuits [9, 11, 13–15, 42]. Although these studies clearly demonstrate the importance of neuronal activity in spine dynamics, the contribution of GABAergic inhibitory transmission known to modulate postsynaptic excitability remains unclear. Here I show that pharmacological blockade of GABA-A receptor-mediated inhibitory transmission with bicuculline results in accelerated spine elimination without affecting new spine formation. Most importantly, spine elimination returns to normal level upon the cessation of blocker administration. These findings indicate that GABA-A receptor-dependent mechanisms curtail spine elimination to prevent spine over-pruning, thereby preserving the integrity of cortical connectivity during naturally occurring circuit refinement. In addition to this role in spine turnover, GABA-A receptors have been shown to control spine morphology. The  $\alpha 1$  receptor subunit deletion



and altered GABA-A receptor membrane trafficking induced by a  $\beta 3$  receptor subunit mutant resulted in the decreased density of mature-looking spines with enlarged spine heads [43, 44]. Thus, normal expression and proper cell surface trafficking of GABA-A receptors contribute to a more stable spine morphology associated with longer persistence within neural circuits. These previous results are consistent with my findings, which support that GABA-A receptor-dependent mechanisms place spine elimination in check to facilitate the global structural stability of cortical excitatory circuits.

Precisely how GABA-A receptors curtail spine elimination to prevent spine over-pruning is not clear. The localization of GABA-A receptors to dendrites and spines makes them well-positioned to influence receptors and channels that mediate many forms of learning- and memory-related synaptic plasticity, including structural plasticity from the losses and gains of spines. N-methyl-D-aspartate (NMDA) receptors are implicated in various aspects of neuronal circuit development. In particular, recent studies have revealed their role in postnatal synaptic refinement. In one study, the elimination of pre-existing spines requires NMDA receptor activity [15]. In addition, low-frequency stimulation of pyramidal neurons in cultured hippocampal slices has been demonstrated to induce rapid spine shrinkage or/and retraction, which is dependent on the activation of NMDA receptors [45, 46]. Consistent with a role for NMDA receptors in synaptic refinement, previous findings have shown reduced elimination of redundant glutamatergic inputs to postsynaptic neurons lacking NMDA receptors in thalamic relay synapses [47]. Taken together, these findings demonstrate that spine/synapse elimination requires NMDA receptor functions. Thus, it is likely that GABA-A receptors influence NMDA receptor activation to prevent excessive spine elimination in circuit refinement. GABA activation of GABA-A receptors generates inhibitory postsynaptic potentials, and this hyperpolarization may enhance the voltage-dependent magnesium block in NMDA receptors, thereby maintaining NMDA receptors in the inactive state. GABA-A receptors might modulate NMDA receptor activation to appropriate levels. Given that spine elimination is dependent on NMDA receptor function, this would place spine elimination in check to prevent excessive spine loss during circuit maturation.

GABA activation of GABA-A receptors controls many aspects of excitatory circuit functions relevant to learning, memory and cognition. My results further indicate that during the extended period of circuit refinement, GABA-A receptors play a critical role in preventing the excessive elimination of spine-based synapses in the neocortex. GABA-A receptor-dependent mechanisms do not appear to affect spine dynamics over a short time interval because bicuculline had no significant effects on spine elimination or formation over a 24-hour duration in preliminary studies. Most importantly, the results from this study showed that enhanced spine elimination following GABA-A receptor blockade (for >1-week duration) occurred at multiple developmental stages over a broad postnatal time interval. The extensiveness of GABA-A receptor effects on spine dynamics during the prolonged period of circuit maturation implicates a role for GABA-A receptor in long-term memory because the long-lasting structural changes from spine losses and gains following behavioral learning processes are thought to provide a structural basis for memory retention. This demonstration of GABA-A receptor-dependent modulation of spine turnover over the long-term has profound implications on the structural stability and overall integrity of cortical

excitatory connectivity critical to learning and memory, and it provides a potential neural mechanism for GABA-dependent regulation of cognitive functions. Furthermore, a wide range of compounds known to modify GABA-A receptor activity have been clinically used for the treatment of neurological, neurodevelopmental and neuropsychiatric conditions. Many of these conditions are indeed associated with dendritic spine pathology and cognitive impairments [48–50]. Thus, the present study supporting GABA-A receptor-dependent mechanisms in promoting circuit integrity provides a structural/cellular basis for the therapeutic effects of GABA-A receptor-targeting agents and contributes to the development of future therapies focused on GABA-A receptor-dependent modulation of spine dynamics.

## Materials and Methods

### Animal

A previously generated mouse line, the YFP-H line, expresses YFP under the control of the *Thy-1* promoter [51]. YFP expression is detected mainly in layer V pyramidal neurons in the cortex of transgenic mice derived from this mouse line [51]. The present study examined the *in vivo* spine dynamics of YFP-labeled layer V pyramidal neurons. In this study, 1-month-old animals (age:  $29.42 \pm 0.38$  days) were re-imaged up to ~4 months of age to investigate spine turnover during a postnatal time period, which is thought to correlate with the time from late childhood to late adolescence/young adulthood in humans. In addition, 4-month-old animals (age:  $4.19 \pm 0.11$  months) were re-imaged up to ~10 months of age to provide spine dynamic profiles during a postnatal stage that most likely correlates with the period from late adolescence/young adulthood to mid-adulthood in humans. Thus, this study established short- and long-term spine dynamic profiles for two distinct postnatal time windows encompassing: (1) 1 to 4 months of age - without overlapping, and (2) 4 to 10 months of age. To determine comparable ages and maturational rates for mouse and human, the current study utilized a reference that the Jackson Laboratory has adapted from Flurkey, et al. [41]: 1 month old in a mouse is equivalent to 12.5 years old in a human, 3 to 6 months old in a mouse is equivalent to 20 to 30 years old in a human, 10 to 14 months old in a mouse is equivalent to 38 to 47 years old in a human, and 18 to 24 months old in a mouse is equivalent to 56 to 69 years old in a human; at 1–6 months of age mice mature 45 times faster than humans, and at > 6 months of age, mice mature 25 times faster than humans. On the basis of a recent study of spine density in humans, the period of late childhood to adolescence correlates to ages of 9 to 22 years [18]. Mice were housed in standard cages with access to water and food *ad libitum*. In addition, animals were housed in groups of 2 to 4 littermates and maintained under light- and temperature-controlled conditions (i.e., 12-hour light-dark cycle at  $22 \pm 2^\circ\text{C}$ ). All but 4 animals used in the study were male. Animals from different litters were used in repeated experiments. All experiments were performed according to the Public Health Service (PHS) Policy on Humane Care and Use of Laboratory Animals and associated guidelines.

For pharmacological experiments, male littermates were injected with either a saline solution or a 0.9% NaCl solution containing bicuculline methiodide (3 mg/kg of body weight; Sigma-Aldrich). Bicuculline was used in this study of GABA-A receptor function at the synapse because it is a general antagonist of GABA-A receptors. Typically, one

intraperitoneal injection was administered on a daily basis. For experiments assessing the reversibility of bicuculline effects, animals received daily saline or bicuculline injection during the first 7 days followed by no injections for the next 7 days prior to the final imaging session. Following bicuculline injection, the animals did not appear to experience any noticeable seizures that may lead to neuronal damage. Any neuronal damage was highly unlikely because spine elimination returned to normal levels upon the cessation of bicuculline administration. Experiments were repeated with male littermates derived from different litters.

## Surgery

For *in vivo* imaging, mice were anesthetized with an initial intraperitoneal injection of ketamine and xylazine in a 0.9% NaCl solution at a dosage of 0.100 mg of ketamine and 0.015 mg of xylazine per gram of body weight. Additional injections of ketamine/xylazine cocktail were administered when necessary. Ketamine is a commonly used anesthetic for transcranial live imaging studies, e.g., [14, 52]. Previous studies have shown that the effects of ketamine on spines are confined to the early postnatal period within the first 2–3 weeks after birth, and that ketamine does not affect *in vivo* spine dynamic at one month of age [53, 54]. This study focused on spine dynamics during postnatal developmental periods after one month of age, which is beyond the critical sensitive time window spanning the first 2–3 postnatal weeks. A ~250- $\mu\text{m}$ -diameter region of the skull overlying the mouse primary somatosensory cortex (stereotactic coordinates: 3.25 mm lateral to the midline and 1.00 mm caudal to bregma) was thinned to ~20- to 30- $\mu\text{m}$  thickness using a high-speed drill and microblades according to a previously described method [55]. Prior to imaging, the skull was glued to a custom-built head mount. This mounting device immobilized the mouse head to greatly reduced breathing-related movements during live imaging. The thinned-skull area was accessible via an opening in the center of the mount. At the completion of the imaging session, the head mount was detached from the mouse head. The animal was then sutured at the open scalp wound area and returned to its home cage.

## High-resolution *in vivo* two photon excitation-based imaging of spines

Transcranial live imaging of the mouse brain through a thinned-skull region was performed using an Olympus BX61WI microscope equipped with a tunable Ti:sapphire laser and a water-immersion objective (60X, 1.1 NA, Olympus). High-magnification image stacks (512  $\times$  512 pixels, 0.170  $\mu\text{m}$ /pixel, 0.7  $\mu\text{m}$  z steps) of spines along the apical dendrites of layer V YFP-labeled pyramidal neurons were acquired with a pulsed 920 nm laser. The maximum laser output power at the sample was set at a range of 10 to 20 mW. For repeated imaging experiments, identification of the previously imaged thinned area was initially performed based on the identification of “landmark” structures (i.e., dendritic branches of interest and blood vessels surrounding these branches) in low-magnification image stacks (512  $\times$  512 pixels, 0.508  $\mu\text{m}$ /pixel, 2.0  $\mu\text{m}$  z steps), and the identification of “landmark” blood vessels in the CCD camera views of the cortical vasculature over the thinned region. In the primary somatosensory cortex of YFP-H transgenic mice, the vast majority of neurons that express YFP are layer V pyramidal neurons. The dendrites and spines under study presumably belonged to layer V YFP-expressing neurons. I imaged dendrites, spines and axons located within the first 100  $\mu\text{m}$  from the pia mater.

## Image analysis

High-magnification image stacks of dendritic branches from transcranial *in vivo* imaging were processed and analyzed using ImageJ. Briefly, 16-bit image stacks were Gaussian filtered, and the resulting image stacks were used for studies of spine dynamics. Only three-dimensional, high-quality image stacks with a signal-to-background-noise ratio of  $> 4$  to 1 were included for analysis. The spines along YFP-labeled dendritic segments were traced manually without prior knowledge of the age and treatment of the animals. Typically, ~15 segments were selected from random locations within the imaged area for spine analysis. Presumably, these dendritic branches are from different parent cells due to the high density of YFP-labeled layer V pyramidal neurons. Dendritic spines were tracked in the three-dimensional stacks instead of the two-dimensional projected images. This was performed to minimize potential errors from movements caused by heartbeat and respiration and the slightly different rotation angles of images between imaging sessions. Classification of dendritic protrusions as “spines” is based on the following criteria: (1) the protrusion length must be  $\geq 1/3$  of the dendritic shaft diameter, (2) the ratio of head diameter to neck diameter must be  $\geq 1.2:1$ , and (3) the ratio of protrusion length to neck diameter must be  $\geq 3:1$ . All other protrusions are considered “filopodia,” which are long and thin structures believed to be spine precursors. Image analysis routinely included all laterally projecting spines on individual dendritic branches.

The images acquired in the beginning and at the end of a specified time interval were compared to determine the appearance or disappearance of spines between the two views. In the two views under study, each spine is considered to be the same spine based on its spatial relationship with neighboring spines and adjacent dendritic and axonal “landmark” structures. For a particular spine under investigation, its position on the dendrite in the second view should not deviate from the expected location for more than  $0.7 \mu\text{m}$ . A spine is considered as a “persisted” spine when it is present in both views over the time interval. For a spine that is present only in the first view, it is determined to be “eliminated” over time. For a spine that is present only in the second view, it is considered to be “added” over time. On the basis of the detailed analysis performed against the initial view, I determined each fraction of spines that “persisted,” “eliminated” and “added” over a specified time frame. In addition, the fraction of spines that survived by the end of a given time frame was calculated as the sum of the percentages of “persisted” and “added” spines.

For figure display only, 2 to 4 consecutive image slices containing an in-focus dendritic branch of interest were first selected from the individual image stack and  $z$ -projected to a two-dimensional image. To clearly show the isolated dendritic branch, the projected image was Gaussian filtered and contrasted. The final image exhibited very few crossing structures and showed all of the elements of the selected dendritic segment.

## Data analysis and statistics

All statistical analyses were performed using SigmaPlot. For multiple group comparisons, significant differences between groups were calculated using Kruskal-Wallis One-Way ANOVA on Ranks followed by a pair-wise multiple comparison procedure (Holm-Sidak’s method). For comparison between two groups, a one-tailed unpaired  $t$ -test was used for data

that passed normality and equal variance tests whereas the Mann-Whitney Rank Sum test was used for non-parametric data. All data are presented as the mean  $\pm$  s.e.m. Significance was defined as  $p < 0.05$ . In the figures, \* denotes  $p < 0.05$ , \*\* denotes  $p < 0.01$ , and \*\*\* denotes  $p < 0.001$ . Linear regression analysis was used to calculate the regression coefficients  $b[0]$ ,  $b[1]$  and  $r^2$  with  $b[1]$  being the slope of the regression line.

## Acknowledgments

I thank Dr. G.-W. Tian, Central Microscopy Imaging Center, Stony Brook University, for assistance with two photon-excitation laser scanning microscopy. I also thank B. Chen for technical assistance and D. Lin for critical reading of the manuscript. This work was supported by the National Institute of Health grant (MH090350).

## References

1. Alvarez VA, Sabatini BL. Anatomical and physiological plasticity of dendritic spines. *Annu Rev Neurosci.* 2007; 30:79–97. [PubMed: 17280523]
2. Bosch M, Hayashi Y. Structural plasticity of dendritic spines. *Curr Opin Neurobiol.* 2012; 22:383–388. [PubMed: 21963169]
3. Chen Y, Sabatini BL. Signaling in dendritic spines and spine microdomains. *Curr Opin Neurobiol.* 2012; 22:389–396. [PubMed: 22459689]
4. Colgan LA, Yasuda R. Plasticity of dendritic spines: subcompartmentalization of signaling. *Annu Rev Physiol.* 2014; 76:365–385. [PubMed: 24215443]
5. Koleske AJ. Molecular mechanisms of dendrite stability. *Nat Rev Neurosci.* 2013; 14:536–550. [PubMed: 23839597]
6. Newpher TM, Ehlers MD. Spine microdomains for postsynaptic signaling and plasticity. *Trends Cell Biol.* 2009; 19:218–227. [PubMed: 19328694]
7. Rochefort NL, Konnerth A. Dendritic spines: from structure to in vivo function. *EMBO Rep.* 2012; 13:699–708. [PubMed: 22791026]
8. Yuste R. Dendritic Spines and Distributed Circuits. *Neuron.* 2011; 71:772–781. [PubMed: 21903072]
9. Hofer SB, Mrsic-Flogel TD, Bonhoeffer T, Hubener M. Experience leaves a lasting structural trace in cortical circuits. *Nature.* 2009; 457:313–317. [PubMed: 19005470]
10. Holtmaat A, Svoboda K. Experience-dependent structural synaptic plasticity in the mammalian brain. *Nat Rev Neurosci.* 2009; 10:647–658. [PubMed: 19693029]
11. Holtmaat A, Wilbrecht L, Knott GW, Welker E, Svoboda K. Experience-dependent and cell-type-specific spine growth in the neocortex. *Nature.* 2006; 441:979–983. [PubMed: 16791195]
12. Kasai H, Fukuda M, Watanabe S, Hayashi-Takagi A, Noguchi J. Structural dynamics of dendritic spines in memory and cognition. *Trends in Neurosciences.* 2010; 33:121–129. [PubMed: 20138375]
13. Trachtenberg JT. Long-term in vivo imaging of experience-dependent synaptic plasticity in adult cortex. *Nature.* 2002; 420:788–794. [PubMed: 12490942]
14. Xu T, Yu X, Perlik AJ, Tobin WF, Zweig JA, Tennant K, Jones T, Zuo Y. Rapid formation and selective stabilization of synapses for enduring motor memories. *Nature.* 2009; 462:915–919. [PubMed: 19946267]
15. Zuo Y, Yang G, Kwon E, Gan WB. Long-term sensory deprivation prevents dendritic spine loss in primary somatosensory cortex. *Nature.* 2005; 436:261–265. [PubMed: 16015331]
16. Anderson B, Rutledge V. Age and hemisphere effects on dendritic structure. *Brain.* 1996; 119(Pt 6):1983–1990. [PubMed: 9010002]
17. Jacobs B, Driscoll L, Schall M. Life-span dendritic and spine changes in areas 10 and 18 of human cortex: a quantitative Golgi study. *J Comp Neurol.* 1997; 386:661–680. [PubMed: 9378859]
18. Petanjek Z, Judas M, Simic G, Rasin MR, Uylings HB, Rakic P, Kostovic I. Extraordinary neoteny of synaptic spines in the human prefrontal cortex. *Proc Natl Acad Sci U S A.* 2011; 108:13281–13286. [PubMed: 21788513]

19. Rivera C, Voipio J, Payne JA, Ruusuvuori E, Lahtinen H, Lamsa K, Pirvola U, Saarma M, Kaila K. The K<sup>+</sup>/Cl<sup>-</sup> co-transporter KCC2 renders GABA hyperpolarizing during neuronal maturation. *Nature*. 1999; 397:251–255. [PubMed: 9930699]
20. Yamada J, Okabe A, Toyoda H, Kilb W, Luhmann HJ, Fukuda A. Cl<sup>-</sup> uptake promoting depolarizing GABA actions in immature rat neocortical neurones is mediated by NKCC1. *J Physiol*. 2004; 557:829–841. [PubMed: 15090604]
21. Barbin G, Pollard H, Gaiarsa JL, Ben-Ari Y. Involvement of GABAA receptors in the outgrowth of cultured hippocampal neurons. *Neurosci Lett*. 1993; 152:150–154. [PubMed: 8390627]
22. Cancedda L, Fiumelli H, Chen K, Poo MM. Excitatory GABA action is essential for morphological maturation of cortical neurons in vivo. *J Neurosci*. 2007; 27:5224–5235. [PubMed: 17494709]
23. Heck N, Kilb W, Reiprich P, Kubota H, Furukawa T, Fukuda A, Luhmann HJ. GABA-A receptors regulate neocortical neuronal migration in vitro and in vivo. *Cereb Cortex*. 2007; 17:138–148. [PubMed: 16452638]
24. LoTurco JJ, Owens DF, Heath MJ, Davis MB, Kriegstein AR. GABA and glutamate depolarize cortical progenitor cells and inhibit DNA synthesis. *Neuron*. 1995; 15:1287–1298. [PubMed: 8845153]
25. Wang DD, Kriegstein AR. GABA regulates excitatory synapse formation in the neocortex via NMDA receptor activation. *J Neurosci*. 2008; 28:5547–5558. [PubMed: 18495889]
26. Farrant M, Nusser Z. Variations on an inhibitory theme: phasic and tonic activation of GABA(A) receptors. *Nat Rev Neurosci*. 2005; 6:215–229. [PubMed: 15738957]
27. Glykys J, Mody I. Activation of GABAA receptors: views from outside the synaptic cleft. *Neuron*. 2007; 56:763–770. [PubMed: 18054854]
28. Mohler H. GABA(A) receptor diversity and pharmacology. *Cell Tissue Res*. 2006; 326:505–516. [PubMed: 16937111]
29. Cobb SR, Buhl EH, Halasy K, Paulsen O, Somogyi P. Synchronization of neuronal activity in hippocampus by individual GABAergic interneurons. *Nature*. 1995; 378:75–78. [PubMed: 7477292]
30. Pouille F, Scanziani M. Enforcement of temporal fidelity in pyramidal cells by somatic feed-forward inhibition. *Science*. 2001; 293:1159–1163. [PubMed: 11498596]
31. Belelli D, Harrison NL, Maguire J, Macdonald RL, Walker MC, Cope DW. Extrasynaptic GABAA receptors: form, pharmacology, and function. *J Neurosci*. 2009; 29:12757–12763. [PubMed: 19828786]
32. Brickley SG, Mody I. Extrasynaptic GABA(A) receptors: their function in the CNS and implications for disease. *Neuron*. 2012; 73:23–34. [PubMed: 22243744]
33. Pirker S, Schwarzer C, Wieselthaler A, Sieghart W, Sperk G. GABA(A) receptors: immunocytochemical distribution of 13 subunits in the adult rat brain. *Neuroscience*. 2000; 101:815–850. [PubMed: 11113332]
34. Fernando RN, Eleuteri B, Abdelhady S, Nussenzweig A, Andang M, Ernfors P. Cell cycle restriction by histone H2AX limits proliferation of adult neural stem cells. *Proc Natl Acad Sci U S A*. 108:5837–5842. [PubMed: 21436033]
35. Nguyen L, Malgrange B, Breuskin I, Bettendorff L, Moonen G, Belachew S, Rigo JM. Autocrine/paracrine activation of the GABA(A) receptor inhibits the proliferation of neurogenic polysialylated neural cell adhesion molecule-positive (PSA-NCAM<sup>+</sup>) precursor cells from postnatal striatum. *J Neurosci*. 2003; 23:3278–3294. [PubMed: 12716935]
36. Fuchs C, Abitbol K, Burden JJ, Mercer A, Brown L, Iball J, Anne Stephenson F, Thomson AM, Jovanovic JN. GABA(A) receptors can initiate the formation of functional inhibitory GABAergic synapses. *Eur J Neurosci*. 2013; 38:3146–3158. [PubMed: 23909897]
37. Huang ZJ, Scheiffele P. GABA and neuroligin signaling: linking synaptic activity and adhesion in inhibitory synapse development. *Curr Opin Neurobiol*. 2008; 18:77–83. [PubMed: 18513949]
38. Chiu CQ, Lur G, Morse TM, Carnevale NT, Ellis-Davies GC, Higley MJ. Compartmentalization of GABAergic inhibition by dendritic spines. *Science*. 2013; 340:759–762. [PubMed: 23661763]

39. Beaulieu C, Colonnier M. A laminar analysis of the number of round-asymmetrical and flat-symmetrical synapses on spines, dendritic trunks, and cell bodies in area 17 of the cat. *J Comp Neurol*. 1985; 231:180–189. [PubMed: 3968234]
40. Chen JL, Villa KL, Cha JW, So PT, Kubota Y, Nedivi E. Clustered dynamics of inhibitory synapses and dendritic spines in the adult neocortex. *Neuron*. 2012; 74:361–373. [PubMed: 22542188]
41. Flurkey, K.; Currer, JM.; Harrison, DE. The Mouse in Aging Research. In: Fox, JG.; Barthold, SW.; Davisson, MT.; Newcomer, CE.; Quimby, FW.; Smith, AL., editors. *The Mouse in Biomedical Research*. Elsevier; Burlington, MA: 2007. p. 637-642.
42. Keck T, Mrcic-Flogel TD, Vaz Afonso M, Eysel UT, Bonhoeffer T, Hubener M. Massive restructuring of neuronal circuits during functional reorganization of adult visual cortex. *Nature Neurosci*. 2008; 11:1162–1167. [PubMed: 18758460]
43. Jacob TC, Wan Q, Vithlani M, Saliba RS, Succol F, Pangalos MN, Moss SJ. GABA(A) receptor membrane trafficking regulates spine maturity. *Proc Natl Acad Sci U S A*. 2009; 106:12500–12505. [PubMed: 19617557]
44. Heinen K, Baker RE, Spijker S, Rosahl T, van Pelt J, Brussaard AB. Impaired dendritic spine maturation in GABAA receptor alpha1 subunit knock out mice. *Neuroscience*. 2003; 122:699–705. [PubMed: 14622913]
45. Nagerl UV, Eberhorn N, Cambridge SB, Bonhoeffer T. Bidirectional activity-dependent morphological plasticity in hippocampal neurons. *Neuron*. 2004; 44:759–767. [PubMed: 15572108]
46. Zhou Q, Homma KJ, Poo MM. Shrinkage of dendritic spines associated with long-term depression of hippocampal synapses. *Neuron*. 2004; 44:749–757. [PubMed: 15572107]
47. Zhang ZW, Peterson M, Liu H. Essential role of postsynaptic NMDA receptors in developmental refinement of excitatory synapses. *Proc Natl Acad Sci U S A*. 2013; 110:1095–1100. [PubMed: 23277569]
48. Korpi ER, Sinkkonen ST. GABA(A) receptor subtypes as targets for neuropsychiatric drug development. *Pharmacol Ther*. 2006; 109:12–32. [PubMed: 15996746]
49. Mohler H. Molecular regulation of cognitive functions and developmental plasticity: impact of GABAA receptors. *J Neurochem*. 2007; 102:1–12. [PubMed: 17394533]
50. Rudolph U, Knoflach F. Beyond classical benzodiazepines: novel therapeutic potential of GABAA receptor subtypes. *Nat Rev Drug Discov*. 2012; 10:685–697. [PubMed: 21799515]
51. Feng G. Imaging neuronal subsets in transgenic mice expressing multiple spectral variants of GFP. *Neuron*. 2000; 28:41–51. [PubMed: 11086982]
52. Grillo FW, et al. Increased axonal bouton dynamics in the aging mouse cortex. *Proc Natl Acad Sci U S A*. 2013; 110:E1514–1523. [PubMed: 23542382]
53. De Roo M, Klauser P, Briner A, Nikonenko I, Mendez P, Dayer A, Kiss JZ, Muller D, Vutskits L. Anesthetics rapidly promote synaptogenesis during a critical period of brain development. *PLoS One*. 2009; 4:e7043. [PubMed: 19756154]
54. Yang G, Chang PC, Bekker A, Blanck TJ, Gan WB. Transient effects of anesthetics on dendritic spines and filopodia in the living mouse cortex. *Anesthesiology*. 2011; 115:718–726. [PubMed: 21768874]
55. Grutzendler J, Kasthuri N, Gan W-B. Long-term dendritic spine stability in the adult cortex. *Nature*. 2002; 420:812–816. [PubMed: 12490949]

### Highlights

- The elimination of pre-existing spines is modulated extensively in mouse postnatal cortical circuit development.
- A substantial decrease in spine elimination decelerates the rate of net spine loss nearly 6-fold beginning at ~4 months of age, a time that is thought to correlate to the transition from late adolescence to young adulthood in humans.
- Pharmacological blockade of GABA-A receptors with bicuculline specifically enhances spine elimination without impacting spine formation.
- This enhancement of spine elimination is reversible upon the cessation of bicuculline treatment.
- Accelerated spine elimination following the functional perturbation of GABA-A receptors can occur at multiple developmental periods during circuit refinement.



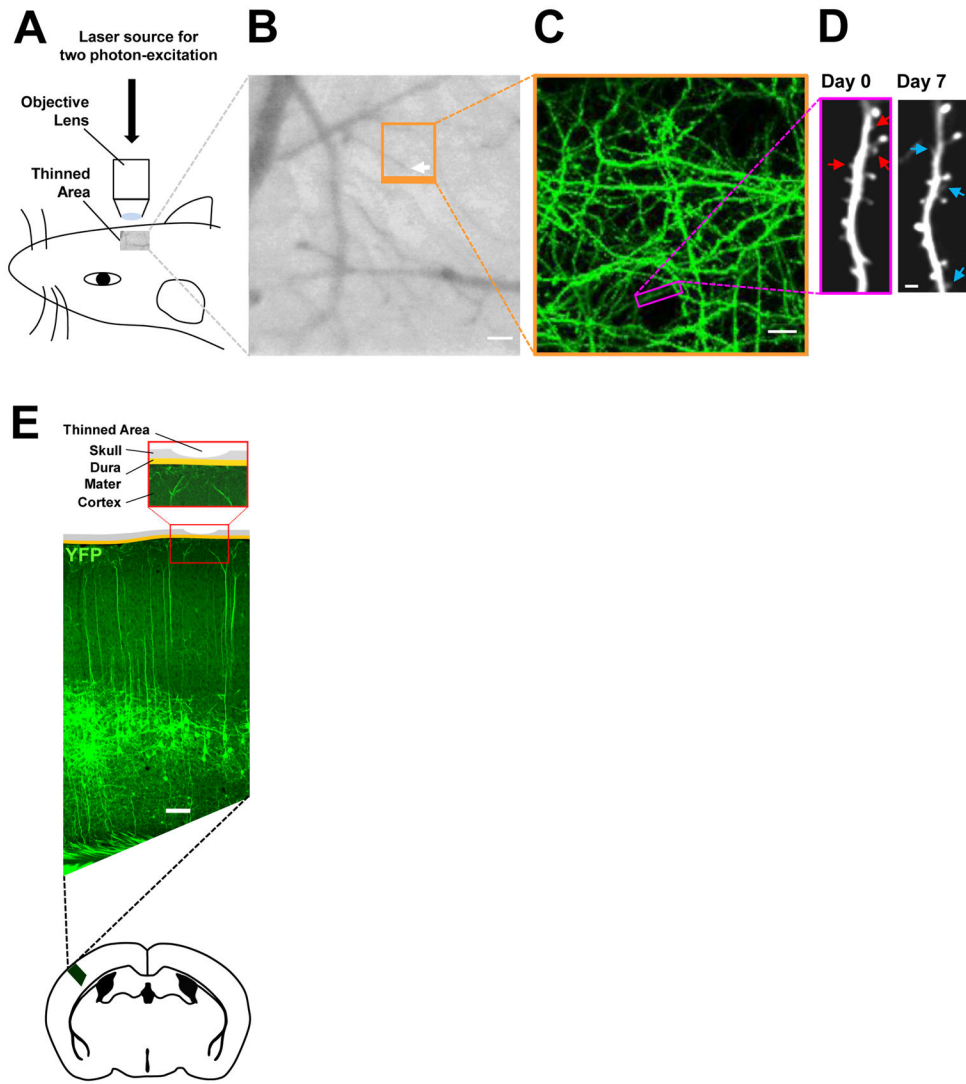


**Figure 1. Live imaging studies of spine dynamics of YFP-labeled layer V pyramidal neurons in the primary somatosensory cortex**

(A) Schematic of transcranial *in vivo* imaging based on two photon-excitation laser scanning microscopy using a pulsed, mode-locked Ti:sapphire laser light source.

(B) CCD camera view of the cortical vasculature beneath a thinned-skull window in a YFP-expressing mouse. The region outlined in orange indicates the area where low- and high-magnification images of dendritic branches were obtained in repeated live imaging. The white arrow points to the tip of a vessel used to relocate the imaged region. Scale bar, 50  $\mu\text{m}$ .

(C) Two-dimensional projection of the low-magnification three-dimensional image stack of dendritic branches and axons from the boxed region in B. A black circular area devoid of YFP (green)-labeled processes in the lower center is the tip of the vessel shown in the boxed region in B. Scale bar, 10  $\mu\text{m}$ .

(D) High-resolution images of a YFP-labeled dendritic segment (box in C) acquired on Day 0 and Day 7. Red arrows indicate pre-existing spines that were eliminated, and blue arrows indicate new spines that were added during the one-week interval. Scale bar, 2  $\mu\text{m}$ .

(E) Schematic of the thinned-skull cranial viewing window preparation for repeated live imaging. Shown is the coronal view of a “thinned-skull” area superposed on to a coronal section of the primary somatosensory cortex of a mouse expressing YFP (green) primarily in layer V pyramidal neurons located deep in the cortex. Scale bar, 100  $\mu\text{m}$ .

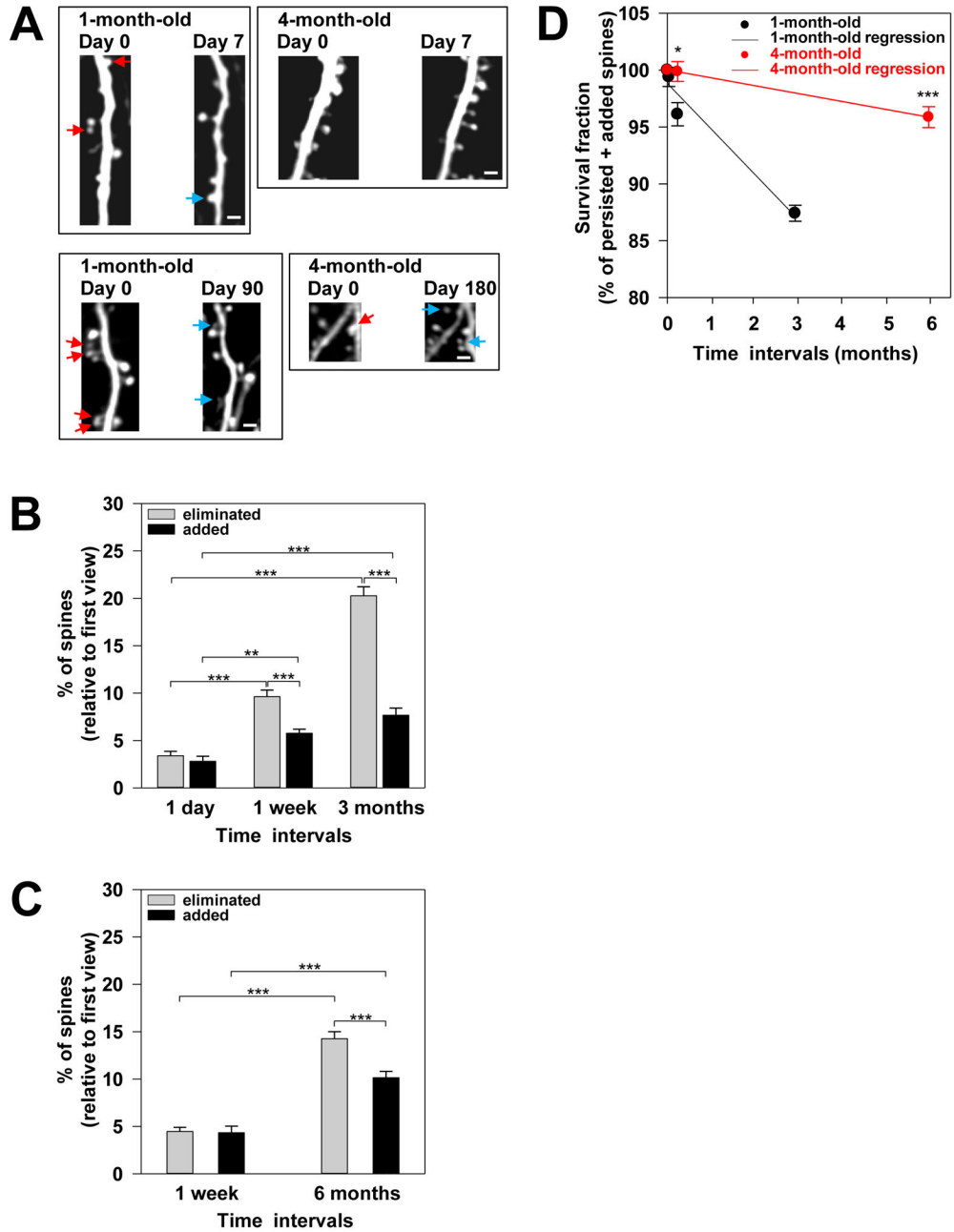


**Figure 2. Long-term *in vivo* imaging studies revealed a nearly 6-fold decrease in the rate of net spine loss within cortical circuits in maturity**  
 (A) Photomicrographs from repeated live imaging of YFP-labeled apical dendritic segments through a thinned-skull cranial viewing window. The red arrows indicate spines that were eliminated over one week (top two panels) and over several months (bottom two panels), respectively, in 1-month-old and 4-month-old mice. The blue arrows indicate new spine that were added over time. Shown are laterally projecting spines on the dendritic segments. Scale bars, 2  $\mu$ m.  
 (B and C) Shown are the percentages of eliminated (gray bars) and added (black bars) spines over the indicated time intervals in 1-month-old (B) and 4-month-old

(C) mice. Statistical analysis was performed using One-Way ANOVA with the Holm-Sidak method for pair-wise multiple comparison. \*\* denotes  $p = 0.012$  and \*\*\* denotes  $p = 0.001$ . Data are presented as the mean  $\pm$  s.e.m.

(D) Survival fractions in 1-month-old (black) animals after one day, one week, and 3 months are shown. In addition, the survival fractions in 4-month-old (red) mice after one week and 6 months are shown. The survival fraction at Day 0 is set at 100%. Regression lines from linear regression analyses are shown for 1-month-old (black, slope= 3.99% per month) and 4-month-old (red, slope= 0.69% per month) animals. Statistical analysis was performed using the Mann-Whitney Rank Sum test. \* denotes  $p = 0.05$  and \*\*\* denotes  $p = 0.001$ . Results are presented as the mean  $\pm$  s.e.m.

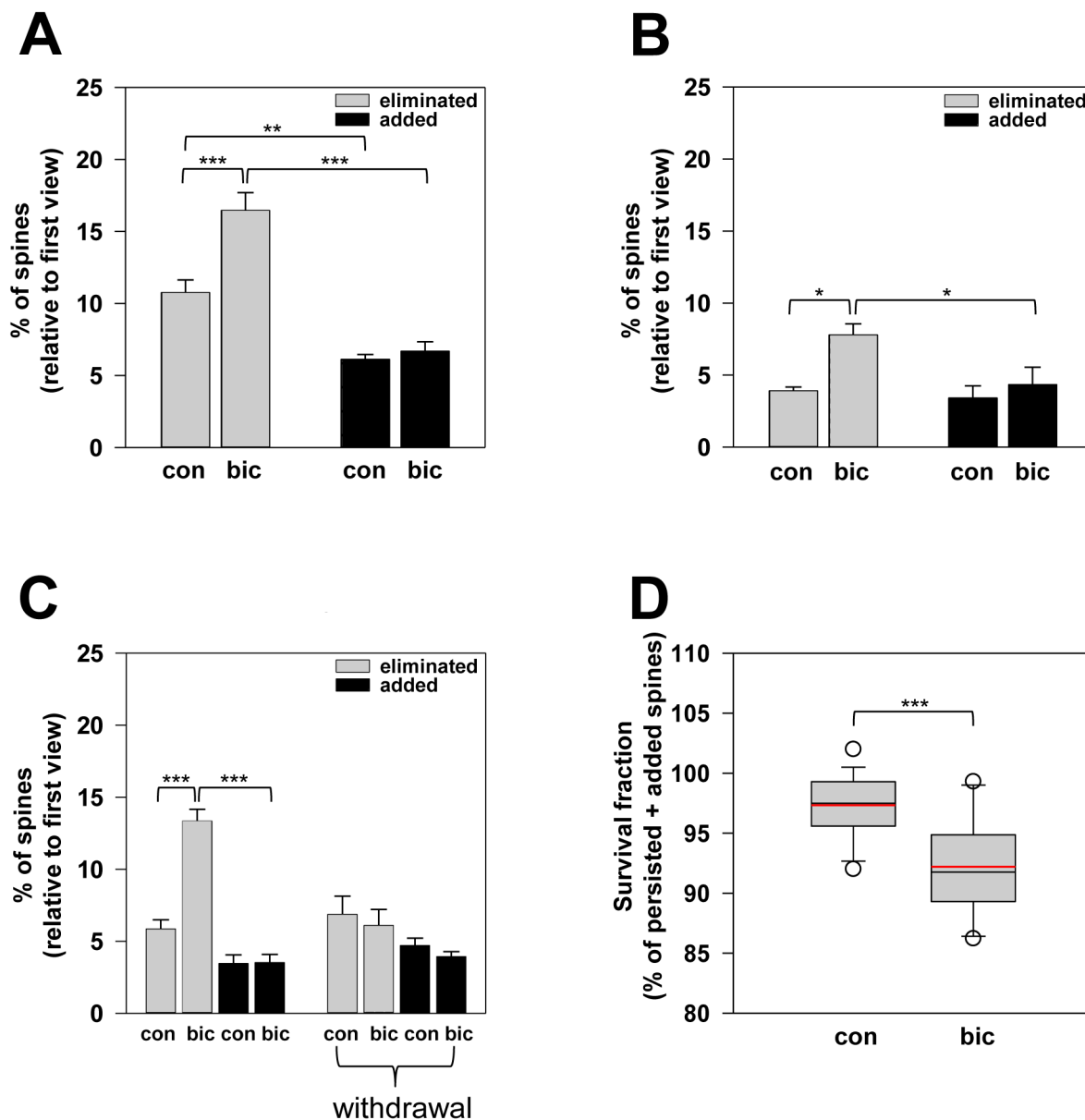


**Figure 3. Bicuculline blockade of GABA-A receptors enhances spine elimination without affecting spine formation**

(A and B) The percentages of eliminated (gray bars) and added (black bars) spines in 1-month-old (A) and 5-month-old (B) mice injected with saline (con) or bicuculline (bic) solution. Statistical analysis was performed using One-Way ANOVA with the Holm-Sidak method for pair-wise multiple comparison. Data are presented as the mean  $\pm$  s.e.m.

(C) Spine dynamics in animals that received daily injections of saline (con) or bicuculline (bic) prior to the final imaging session are shown. In addition, spine dynamics in animals subjected to the withdrawal experimental paradigm (denoted with “withdrawal”) are shown. For these animals, daily injections of saline (con) and bicuculline (bic) were administered for the first 7 days followed by no injections for the next 7 days prior to the final view.

Statistical analysis was performed using One-Way ANOVA with the Holm-Sidak method for pair-wise multiple comparison. Data are presented as the mean  $\pm$  s.e.m.

(D) Survival fractions of spines in saline- (con) and bicuculline-treated (bic) mice. The box plot shows the extreme values, the 25% and 75% percentiles, medians and error bars. The mean lines are displayed in the plot in red. Statistical analysis was performed using Student's one-tailed unpaired *t*-test.